Application of Taguchi Method to Robust Design of Acoustic Performance in IMT-2000 Mobile Phones

Gun-Yong Hwang[1], Sang-Moon Hwang[2], Hong-Joo Lee[2], Ji-Hoon Kim[2], Keum-Shik Hong[2], and Won-Yeoul Lee[1]

[1]Department of Information and Communication Engineering, Youngsan University, Kyoungnam 626-847, Korea
[2]School of Mechanical Engineering, Pusan National University, Keumjung-gu, Busan 609-735, Korea

This paper describes an approach to design of acoustic devices, such as microspeaker and dynamic receiver, considering the acoustic characteristics improvement in IMT-2000 mobile phones. The analysis of a newly designed microspeaker considering mechanical, electrical, and magnetic coupling effects is performed using the finite-element method (FEM) and its validity is confirmed as well by experiments. Also, a statistical approach is suggested to identify a certain relationship between a mobile phone and a newly designed microspeaker. The approach is based on the Taguchi method and utilizes the orthogonal array for design of experiments (DOE). The concept of signal-to-noise (S/N) ratio is applied to evaluate the acoustic performance in mobile phones.

***Index Terms*—Acoustic characteristics, coupling, finite-element method, IMT-2000, microspeaker, SPL, Taguchi method.**

I. INTRODUCTION

HIGH-PERFORMANCE microspeakers with broad-band frequency are essential for multimedia function in IMT-2000 mobile phones. With the increased size of multimedia liquid crystal display (LCD) window, space for microspeakers is relatively reduced to maintain the same phone size. Moreover, for acoustic parts, such as a microspeaker and a dynamic receiver, smaller size and lighter weight are relatively difficult to realize compared to electronic parts, since size and weight are closely related to the acoustic performance. One possible way of achieving size reduction is to integrate two parts within one device. Fig. 1(a)–(c) shows schematics of conventional microspeakers and the integrated device that has been newly designed in this paper.

The integrated device is the type that combines conventional inner permanent-magnet (PM) microspeaker and conventional outer PM microspeaker. It is noted that a receiver has nearly the same configuration as a microspeaker except for the electrical impedance. The integrated device is similar in diameter and thickness to each conventional type, because the magnetic circuit and the vibration space are shared within a structure.

Fig. 1(d) shows the attached layout of the integrated device when it is mounted on the folder-type mobile phone. With folded status, the speaker is to generate a paging melody. With unfolded status, the receiver is to function for communication.

This paper introduces the integrated device that has an advantage in mounting space over conventional type. For sound pressure level (SPL) analysis, electromagnetic, mechanical, acoustic, and their coupling effects are considered. Results show that the integrated devices have equivalent performance compared with the conventional microspeakers with similar surface area. Finally, a statistical approach to achieve high characteristics and performance is suggested by Taguchi methods to identify a certain relationship between a mobile phone and a designed microspeaker.

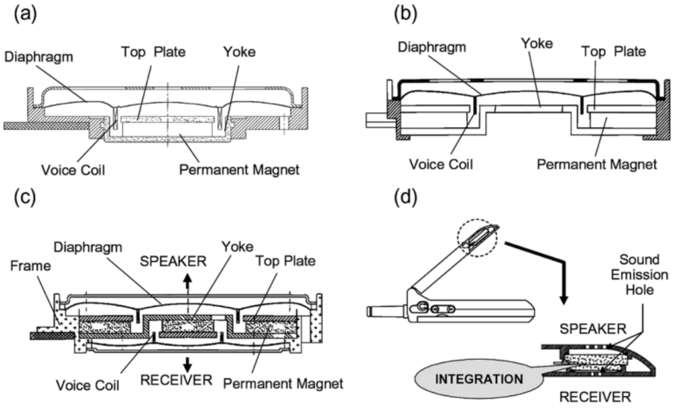

Fig. 1. Schematic of the devices and mounting layout: (a) Conventional inner PM speaker. (b) Conventional outer PM speaker. (c) Integrated device. (d) Mounting layout of the integrated device.

II. DESIGN OF MICROSPEAKER

A. Method of Analysis

A top plate helps to concentrate most of the magnetic flux within the permanent magnet into the narrow radial gap. A time-varying current from an amplifier drive is fed into a voice coil attached to a diaphragm. The diaphragm motion is free to move predominantly in the axial direction. For the electromagnetic field analysis, a two-dimensional finite-element method (FEM) can be implemented utilizing axisymmetric boundary condition. The governing equation describing the electromagnetic system can be derived from Maxwell's equations. The magnetic flux density $\vec{B}$ can be expressed as the curl of the magnetic vector potential of $\vec{A}$ as in (1)

$$\vec{B} = \nabla \times \vec{A}. \tag{1}$$

In the case of low frequencies and quasi-static field, magnetic fields can be described by the partial differential equation as in (2)

$$\nabla \times \left(\frac{1}{\mu} \nabla \times \vec{A} \right) = \vec{J} \tag{2}$$

Digital Object Identifier 10.1109/TMAG.2005.846255

where $\vec{J}$ and μ denote the current density and the permeability. Voice-coil current can be also determined by solving voltage equation of the equivalent circuit as in (3), where V, R, I, and L denote applied voltage, coil resistance, coil current, and inductance, respectively. The voice-coil motion generates the back electromotive force (EMF) $Bl(z)\dot{z}$, where l, z, and $\dot{z}$ are the voice-coil length, the voice-coil displacement, and velocity. The magnetic exciting force resulting from the interaction between the magnetic field and the total electric currents can be expressed as in (4)

$$V = IR + L\frac{dI}{dt} + Bl(z)\dot{z} \tag{3}$$

$$F_{\text{coil}} = \oint Idl \times B. \tag{4}$$

The mechanical model of the vibrating diaphragm including voice coil can also be developed using FEM. Displacement and surface velocity of the diaphragm can be obtained by solving mechanical vibration equation as in (5), where $[M], [C], [K]$, and $\{F_{\text{coil}}(t)\}$ denote mass matrix, damping coefficient matrix, stiffness coefficient matrix, and magnetic exciting forces acting on voice coil, respectively

$$[M]\{\ddot{z}\} + [C]\{\dot{z}\} + [K]\{z\} = \{F_{\text{coil}}(t)\}. \tag{5}$$

Assuming a free acoustic field for an acoustical analysis, the propagation of an acoustic wave in a homogeneous nonviscous fluid medium is governed by the linear wave equation as in (6)

$$\nabla^2 p = \frac{1}{c^2}\frac{\partial^2 p}{\partial t^2} \tag{6}$$

where p and c are acoustic sound pressure and wave speed, respectively. The sound power radiated by a microspeaker vibrating in a mean rms surface with the spatial velocity of $\langle V_0^2(f)\rangle$, can be calculated as in (7)

$$W_{\text{rad}}(f) = \rho c S_{\text{rad}} \sigma_{\text{rad}}(f) \langle V_0^2(f)\rangle \ [\text{W}] \tag{7}$$

where $f, \rho, c, S_{\text{rad}}$, and σ_{rad} are the frequency of vibration, density of the air, the velocity of the propagation of sound in air, area of the diaphragm surface contributing to sound radiation, and the radiation efficiency, respectively. The sound radiation efficiency is calculated by a simplified equation, in which the diaphragm is considered as a monopole source, and is given as in (8), [1]

$$\sigma_{\text{rad}}(f) = \frac{k^2a^2}{1 + k^2a^2} \tag{8}$$

where $k = 2\pi f/c$ is the wavenumber and a is the diaphragm radius. The SPL at distance d from the source can be expressed as in (9)

$$L_p(d) = L_w - 20\log\left(\frac{d}{d_o}\right) - 8 \ [\text{dB}] \tag{9}$$

where L_w is the sound power level as in (10), and the normalized value for d_o is 1 m

$$L_w(d) = 10\log\left(\frac{W_{\text{rad}}}{10^{-12}}\right) \ [\text{dB}]. \tag{10}$$

Fig. 2 shows the overall analysis procedure in which the given system is to be decoupled [2].

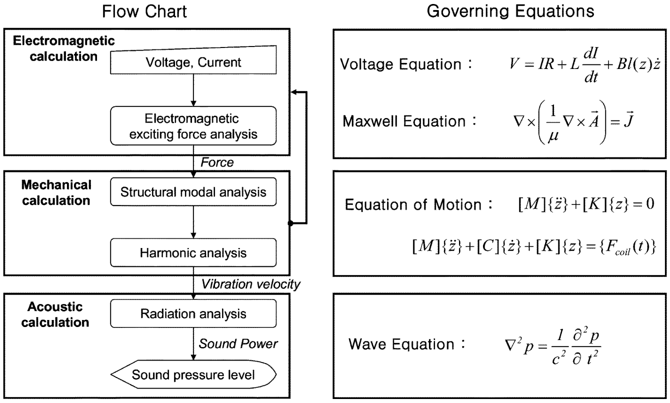

Fig. 2. Flowchart of a decoupling procedure.

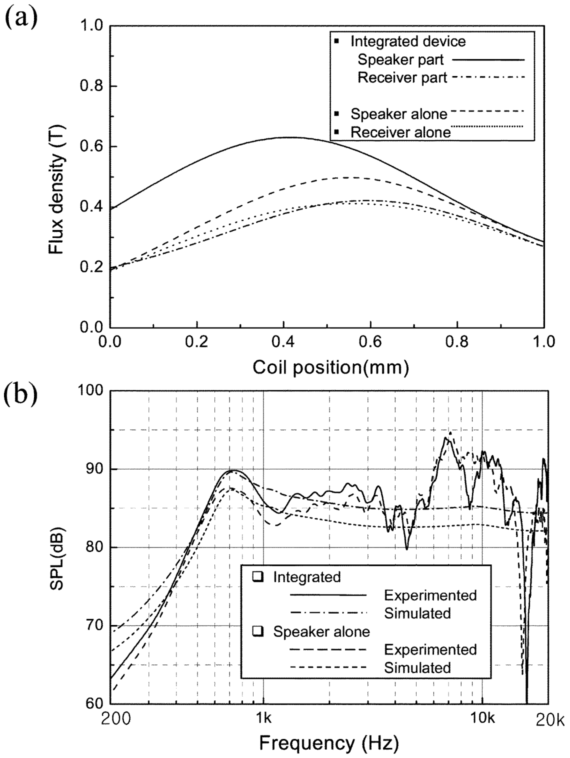

Fig. 3. Magnetic flux density and SPL. (a) Magnetic flux density in air gap. (b) SPL of the speakers.

B. Results and Discussions

Fig. 3(a) shows magnetic flux density at air gap and integrated device shows increased flux density. This is due to the increased magnet volume of the ring-type outer PM of the integrated device. Fig. 3(b) shows speaker SPL characteristics for a speaker alone and an integrated device. Simulated and experimental results are also compared and show good agreement especially at important frequency region of the speaker, 500 Hz–2 kHz. Some discrepancy at higher frequency region results from the complicated acoustic impedance characteristics of surface hole of the microspeakers. The speaker of the integrated device shows improved performance due to efficient magnetic circuit design and increased magnet volume and the receiver, as well. Table I shows the comparison of specifications of the devices.

TABLE I
SPECIFICATIONS OF DEVICES

	Speaker alone	Receiver alone	Integrated device	
			Speaker part	Receiver part
Diameter [mm]	15	13	15	12
Thickness[mm]	3.5	2.5	3.7	
Max SPL [dB]	86	120	90	120
1st resonance frequency [Hz]	700	650	720	550

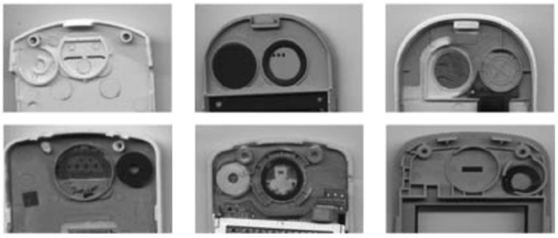

Fig. 4. Various phone-cases for mobile phones.

III. IDENTIFICATION OF COUPLING CHARACTERISTICS BETWEEN A MOBILE PHONE AND A MICROSPEAKER

For a realistic application, even a high-performance microspeaker may not achieve its design characteristics when mounted onto a mobile phone-case due to acoustic impedance mismatch. Therefore, coupling relationship between a mobile phone and a microspeaker should be considered for mass production. Fig. 4 shows various phone-cases for mobile phones. In this section, coupling relationship is considered by the Taguchi method. Taguchi methods were developed by Genichi Taguchi to improve the implementation of total quality control in Japan. They are based on the design of experiments to provide near optimal quality characteristics for a specific objective. The real power of Taguchi methods comes from their simplicity of implementation [3], [4]. The goal is not just to optimize an arbitrary objective function, but also to reduce the sensitivity of engineering designs to uncontrollable factors or noise. In IMT-2000 mobile phones, it is necessary to adopt a broad-band microspeaker to realize multimedia communication. Using the predesigned prototype, the following two case studies have been done for the realistic application.

A. Case 1—Experiment and Analysis for Maximize SPL at 1024 Hz

1) Define Problem: Case 1 deals with a problem to maximize SPL at 1024 Hz. In this case, the melody of a mobile phone sounds loudest.

This case study is larger-is-better problem in which higher SPL is better. In this experiment, signal-to-noise (S/N) ratio is suggested as a measure of improvement of SPL. Therefore, optimal condition is to be determined by choosing high S/N ratio in each level.

2) Identification of Major Design Factors: Factors that affect SPL curve are classified into control factors and noise factors by experiment. Measured response (y_i) is chosen as SPL measured at 1024 Hz in SPL curve. According to each control factor, each level has been set up. Consequently, seven control factors and one noise factor are chosen. Table II shows composition of each factor to be used in experiment array.

TABLE II
FACTORS FOR EXPERIMENT LAYOUT

Factor	Sym.	Content	Level 1	Level 2	Level 3
Control	A	Mock-up sealing level	Full sealing	Half sealing	X
	B	Poron type	Poron A	Poron B	X
	C	Mock-up shape	Cylinder	Semi-cylinder	Hexahedron
	D	Mock-up volume	10cc	5cc	3cc
	E	Poron thickness	Thick	Thin	Without poron
	F	Size of sound hole	Large	Middle	Small
	G	Screen type	Screen A	Screen B	Without screen
Noise	N	Surrounding	Quiet		Noisy

TABLE III
ORTHOGONAL ARRAY LAYOUT OF $L_{36}(2^2 \times 3^5)$ TYPE

Exp. No.	Inner array (control factors)							Outer array (noise factor)			
								N1		N2	
	A	B	C	D	E	F	G	R1	R2	R1	R2
1	1	1	1	1	1	1	1	85.155	85.1776	84.8102	84.9613
2	1	1	2	2	2	2	2	86.4528	86.3384	86.0785	86.2967
3	1	1	3	3	3	3	3	71.5856	72.0901	72.0854	72.3914
4	1	1	1	1	1	1	2	84.9254	84.6351	84.6233	84.7001
5	1	1	2	2	2	2	3	86.2863	86.2104	86.2809	86.2276
:	:	:	:	:	:	:	:	:	:	:	:
31	2	2	1	3	3	3	2	63.8162	63.3154	62.8639	63.6214
32	2	2	2	1	1	1	3	86.9341	87.021	86.7994	86.8059
33	2	2	3	2	2	2	1	91.8014	91.6655	91.5595	91.6725
34	2	2	1	3	1	2	3	84.5152	84.3353	84.2555	84.3105
35	2	2	2	1	2	3	1	81.187	80.9971	81.2845	81.1242
36	2	2	3	2	3	1	2	78.7703	78.6587	78.4341	78.5296

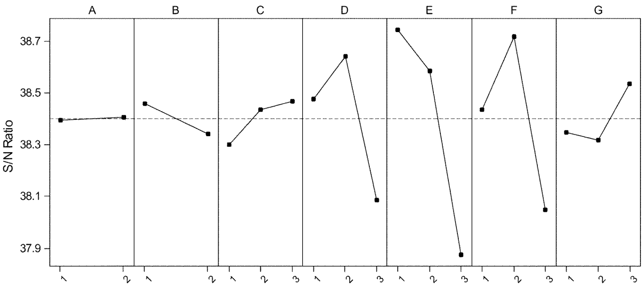

Fig. 5. Graph of analysis result. (Analysis for maximize SPL).

3) Table of Orthogonal Arrays and Experiment: Since there are two control factors in level 2 and five in level 3, $L_{36}(2^2 \times 3^5)$ inner array is set up. Noise factors in outer array are divided into two cases; when surroundings are quiet and noisy. Experiments have been performed twice in random order every 30 min. Orthogonal array for the experiment is shown in Table III.

4) Start Analysis: With the previous results, statistical analysis is performed using MINITAB R13. S/N ratio is shown in Fig. 5.

TABLE IV
COMPARISON OF S/N RATIO ESTIMATE

	Level 1	Level 2	Level 2 or 3	Optimal condition
S/N ratio	38.7511	39.0418	37.3579	39.5686

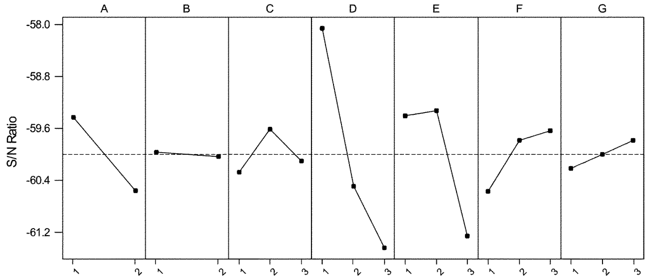

Fig. 6. Graph of analysis result. (Analysis for lowering the first natural frequency).

TABLE V
COMPARISON OF S/N RATIO ESTIMATE

	Level 1	Level 2	Level 2 or 3	Optimal condition
S/N ratio	-57.9248	-59.8262	-62.8476	-55.8181

5) Optimal Condition: Choosing factors with high S/N ratio, A2, B1, C3, D2, E1, F2, and G3 are the optimal condition. However, such factors, like A and B, give no effect on the optimal condition while E, F, and D are the ones that affect the optimal conditions most. Good combination of proper levels for E, F, and D can lead to an equivalent condition to the optimal condition. With these results, it is possible to suggest a design standard for the improvement of SPL.

6) Prediction of Taguchi Result: Using evaluation technique, comparison of estimated S/N ratio in each level and in optimal condition is shown. The result is listed in Table IV showing that the optimal estimate is larger than other estimates in each level.

In the result, the optimal condition shows improved S/N ratio by $0.8175(39.5686 - 38.7511)$. This reduces loss cost by $1.207(10^{0.08175})$ times when converted into money. Therefore, it can be said that mounting a microspeaker onto a mobile phone according to the optimal condition can higher SPL at 1024 Hz by 1.207 times compared to the level 1.

B. Case 2—Experiment and Analysis for Lowering the First Natural Frequency

This experiment shows a case study to find out a method that lowers the first natural frequency in mounting a microspeaker onto a mobile phone. This case study is smaller-is-better problem in which lower natural frequency is better. The analysis procedure is the same as case 1. S/N ratio is shown in Fig. 6. The result shows that, A1, B1, C2, D1, E2, F3, and G3 are the optimal condition when high S/N ratio was chosen. Comparison of estimated S/N ratio in each level and optimal condition is shown in Table V.

In the result, the optimal condition shows improved S/N ratio by $2.1067(-55.8181 + 57.9248)$. This reduces loss cost by $1.6243(10^{0.21067})$ times when converted into money. Therefore, it can be said that mounting a microspeaker onto a mobile phone according to the optimal condition can lower the first natural frequency by 1.624 times compared to the level 1.

IV. CONCLUSION

The size reduction of IMT-2000 mobile phones still remains the most prominent trend in the marketplace and demands a continual effort for the size reduction of components. The most realistic approach for size reduction is accompanied by integrating two parts within a structure. This paper introduces a new design of integrated speaker and receiver using electromagnetic, mechanical, acoustic, and magnetic coupling analysis. Results show that the proposed type shows better performance maintaining the similar diameter and thickness. The Taguchi method has been implemented to identify coupling effects between a microspeaker and a mobile phone. Through comparison of various experimental conditions, optimal condition to maximize SPL at 1024 Hz has been obtained and optimal condition to lower the first natural frequency as well. Obtained optimal conditions can be effectively used as a design standard for a phone-case design.

APPENDIX

The S/N ratios are used as the selection criteria for control factor level selection. In general, the largest S/N ratio identifies minimum variance relative to some mean value

$$\mathrm{SN}_{\mathrm{Larger-is-better}} = -10\log_{10}\frac{1}{n}\sum_{i=1}^{n}\frac{1}{y_i^2}$$

$$\mathrm{SN}_{\mathrm{Smaller-is-better}} = -10\log_{10}\sum_{i=1}^{n}\frac{y_i^2}{n}$$

where y_i and n are the measured response and the number of measurements, respectively.

ACKNOWLEDGMENT

This work was supported by the National Research Laboratory, Ministry of Science and Technology, Korea, under Grant NRL M1-0302-00-0039-03-J00-00-023-10.

REFERENCES

[1] L. E. Kinsler, *Fundamentals of Acoustics*. New York: Wiley, 1982.
[2] G. Y. Hwang, H. J. Lee, S. M. Hwang, B. S. Kang, and S. K. Jeung, “Performance comparison between inner and outer permanent magnet type micro-speakers used for mobile phones,” *J. Appl. Phys.*, vol. 93, no. 10, pp. 8519–8521, 2003.
[3] A. N. Link and G. Tassey, “Propulsion system design optimization using the Taguchi method,” *IEEE Trans. Eng. Manage.*, vol. 40, no. 3, pp. 315–322, Aug. 1993.
[4] S. Brisset, F. Gillon, S. Vivier, and P. Brochet, “Optimization with experimental design: An approach using Taguchi’s methodology and finite element simulations,” *IEEE Trans. Magn.*, vol. 37, no. 5, pp. 3530–3533, Sep. 2001.

Manuscript received June 8, 2004.